arXiv:astro-ph/0004116v1 8 Apr 2000

THE GLOBULAR CLUSTER SYSTEM IN THE INNER REGION OF THE GIANT ELLIPTICAL GALAXY NGC 4472

Myung Gyoon Lee and Eunhyeuk Kim
Astronomy Program, SEES, Seoul National University, Seoul 151-742, Korea
Email: mglee@astrog.snu.ac.kr, ekim@astro.snu.ac.kr

ABSTRACT

We present a study of globular clusters in the inner region of the giant elliptical galaxy NGC 4472, based on the *HST* WFPC2 archive data. We have found about 1560 globular cluster candidates at the galactocentric radius $r < 4$ arcmin, most of which are located within $r = 1.1$ arcmin. $V-(V-I)$ diagram of these objects shows a dominant vertical structure which consists obviously of two components: blue globular clusters (BGCs) and red globular clusters (RGCs). The luminosity function of the globular clusters is derived to have a peak at $V(\mathrm{max}) = 23.50 \pm 0.16$ mag and $\sigma = 1.19 \pm 0.09$ from Gaussian fitting. From this result the distance to NGC 4472 is estimated to be $d = 14.7 \pm 1.3$ Mpc, for the foreground reddening $E(V-I) = 0.03$ and the peak luminosity for the Galactic globular clusters of $M_V(\mathrm{max}) = -7.4$ mag. The peak luminosity for the RGCs is similar to that for the BGCs, which indicates that the RGCs may be several Gyrs younger than the BGCs. The luminosity function of the globular clusters shows little systematic variation depending on the galactocentric radius at $r < 4$ arcmin. However, the mean luminosity of the bright BGCs decreases by 0.2 mag with increasing galactocentric radius over the range of 9 arcmin, while that of the RGCs does not. The observed color distribution of these globular clusters is distinctively bimodal with peaks at $(V-I) = 0.98 \pm 0.01$ and 1.23 ± 0.01, which correspond to the metallicities of [Fe/H] $= -1.41$ and -0.23 dex, respectively. The mean observed color of all the globular clusters with $V < 23.9$ mag is derived to be $(V-I) = 1.11 \pm 0.01$ (m.e.), corresponding to the metallicity of [Fe/H] $= -0.79 \pm 0.05$ dex. These colors are exactly the same as those for the globular clusters in M87. It is found that the relative number of the BGCs to the RGCs is increasing with the increasing galactocentric radius. There are more RGCs than the BGCs within $r \sim 2$ arcmin, while there are fewer RGCs than the BGCs in the outer region of NGC 4472. Radial and azimuthal structures of the globular cluster system in NGC 4472 are also investigated. Surface number density profiles of both the BGCs and RGCs get flat in the central region, and the core radii of the globular cluster systems are measured to be $r_c = 1.9$ arcmin for the BGCs, $r_c = 1.2$ arcmin for the RGCs, and $r_c = 1.3$ arcmin for the total sample, which are much larger than the stellar core of the galaxy. In general the properties of the globular clusters in the inner region of NGC 4472 are consistent with those of the globular clusters in the outer region of NGC 4472.

Subject headings: galaxies: individual (NGC 4472) – galaxies: star clusters – galaxies: abundances – galaxies: photometry — Distance scale – globular clusters: general

1. INTRODUCTION

NGC 4472 (M49) is a giant elliptical galaxy located at 4° south of the center of the Virgo cluster. NGC 4472 is the brightest member of the Virgo cluster, some 0.2 mag brighter than the cD galaxy M87. NGC 4472 is an outstanding example of giant elliptical galaxies showing a bimodality in the color distribution of globular clusters (Gebhardt & Kissler-Patig 1999, Kundu 1999). Geisler, Lee, & Kim (1996) and Lee, Kim, & Geisler (1998) have found from the deep wide (16.4×16.4 arcmin^2) field CCD imaging of NGC 4472 that the color distribution of the globular clusters in NGC 4472 is remarkably bimodal. The bimodal color distribution of the globular clusters in NGC 4472 has shown that there are two kinds of cluster populations in this galaxy: a metal-poor population with a mean metallicity of [Fe/H] $= -1.3$ dex and a metal-rich population with a mean metallicity of [Fe/H] $= -0.1$ dex. Interestingly it is found that the metal-rich globular clusters show some properties in common with the galaxy halo stars in their spatial distribution and color profiles, while the metal-poor globular clusters do not show such behavior. Also it is found that the metal-rich globular clusters are more centrally concentrated than the metal-poor globular clusters. This result indicates that there may exist some connection between the metal-rich globular clusters and halo stars in NGC 4472 in the formation and evolution processes. However, these studies based on the ground-based observations could not investigate the properties of the globular clusters close to the center of NGC 4472, because of the severe crowding problem and strong background halo light in ground-based images of the inner region of the galaxy. Hubble Space Telescope (HST) data are ideal for the study of the globular clusters close to the center of bright galaxies such as NGC 4472. They are especially useful for the study of the structure of the globular cluster system in the central region of NGC 4472 for which little is known by now.

In this paper we present a study of the globular clusters in the inner region of NGC 4472 using the HST archive data. During the preparation of this paper Puzia et al. (1999) published a paper based on the analysis of the data which are the same as three sets among the four sets used in this study. However, there are several differences between the two studies, details of which will be described later. Here is given a brief summary of the differences between the two studies. First, we use one more data set in addition to the data set used by Puzia et al., with which the size of the bright globular cluster sample is increased by 29% and the complete areal coverage of the bright globular cluster sample is increased significantly (by a factor of three in the range of the galactocentric radius). Secondly, we use different methods of data reduction and analysis from the Puzia et al.'s. As a result, our photometry goes about 1 mag deeper and is more complete than the Puzia et al.'s before incompleteness correction. Third, V and I magnitudes in our photometry are on average about 0.2 mag fainter than the Puzia et al.'s for the common objects, while the colors are almost the same between the two studies. Fourth, our results for the peak luminosity of the globular cluster luminosity functions are significantly different from the Puzia et al.'s, leading to an opposite conclusion on the age of the globular clusters. Fifth, we present for the first time a study of the structure of the central region of the globular cluster systems which was not done by Puzia et al. Sixth, we use both the HST data of the inner region of NGC 4472 and the ground-based data of the outer region of NGC 4472 to investigate any systematic variation over a wide range, while Puzia et al. worked with only the HST data of the inner region.

This paper is composed as follows. Sections 2 describes the data used in this study, and 3 explains the reduction of the data. Section 4 presents the color-magnitude diagram of the measured objects in the NGC 4472 field. Sections 5 and 6 show, respectively, the luminosity functions and color distribution of globular clusters. Section 7 investigates the spatial structure of the globular cluster system in NGC 4472. Primary results are discussed in Section 8, and a summary of this study is given in the final section.

2. DATA

We have used four sets of HST Wide Field and Planetary Camera 2 (WFPC2) imaging data on NGC 4472 available in the HST archive for this study: two fields including the center of NGC 4472, one field 3 arcmin north, and one field 3 arcmin south from the center of NGC 4472. We name these HST fields: C1 Field, C2 Field, N Field and S Field. The images were obtained with the wide-band filters F555W and F814W. Table 1 lists the observation log of these data and Fig. 1 displays the positions and orientations of the HST fields in the digitized Palomar Sky Survey

image of NGC 4472. Areal coverage of the data used in this study extends out to $r \approx 4$ arcmin, and is almost complete inside $r = 1.1$ arcmin.

3. DATA REDUCTION

3.1. Image Processing

C1 and C2 Fields include the nucleus of NGC 4472 so that the background halo light is much brighter than the globular clusters in the images. Therefore we need to subtract the galaxy halo light before doing photometry of the point sources in the images.

We first construct smooth models of halo light using ellipse fitting and median smoothing, then subtract these models from the original images. The subtraction works very well and the resulting images show clearly the point sources close to the center of NGC 4472. Cosmic rays in the images were removed and individual images of the same filter were combined into a single image using CRREJ task in IRAF/STSDAS.

3.2. Aperture Photometry

Crowding problem of the point sources seen in the *HST* images of NGC 4472 is negligible so that simple aperture photometry is good enough to derive reliable photometry of point sources. We have obtained the photometry of point sources in the images as follows.

First, we find objects with 4 σ threshold from the images prepared by combining all F555W and F814W images, using FIND in IRAF/DAOPHOT. Secondly, we derive aperture magnitudes of these objects from the combined images of each filter. For this we use CCDCAP designed for accurate aperture photometry of point sources in the *HST* images (Mighell 1998). We use the aperture radius of 2 pixels, the sky radius of 5–8 pixels, and the hardness parameter of 0.8 in CCDCAP. Thirdly, we derive the aperture corrections for the aperture radius of 0.5 arcsec using the bright point sources (which are mostly globular clusters) in each image, the results of which are listed in Table 2. Finally we derive standard magnitudes and colors of these objects following the description given in Holtzman et al. (1995a, b) and Kundu et al. (1999). We adopt the zero points of the magnitudes given in Holtzman et al. (1995a, b). We have tried to measure the excess light of bright globular clusters compared with the stellar point spread function over the aperture region larger than the radius of 0.5 arcsec, as Puzia et al. did. However, it is found that it is not possible to measure reliably the amount of the excess light, because of low signal-to-noise ratios for the outer region. The final photometry reaches $V \sim 28$ mag, and the total number of objects in the photometry list is about 5670.

It is not easy to secure reliable photometry of the objects in the *HST* WFPC2 images as ours, especially due to difficulty in measuring the sky value and deriving the aperture correction. Fortunately we can check the accuracy of the photometry using the objects located in the overlapped region among the *HST* fields. C2 field (that was not used by Puzia et al. 1999) is overlapped with C1 field and N field so that it is very useful for checking externally the accuracy of the photometry of C1 and N fields. Table 3 and Fig. 2 show the comparison of the photometry for the point sources common among the *HST* fields. In general the photometry of the objects show good agreement among the overlapped fields, and the mean differences of the photometry for the total sample are $\Delta V = 0.001 \pm 0.049$ (N = 52) and $\Delta I = -0.026 \pm 0.051$ (N = 59). This result shows that the sky measurement and aperture correction in our photometry are reliable.

3.3. Image Classification

There are included both point sources and extended sources in the list of the detected objects, and these are foreground Galactic star, globular clusters in NGC 4472, or background galaxies. Here we mean galaxies by extended sources, and mean stars and globular clusters (even though they are somewhat resolved) by point sources. Point sources are indeed mostly globular clusters rather than stars, as will be shown later. We have selected point sources from the list of the detected objects using the morphological classifier r_{-2} moment, an indicator for the degree of central concentration of light of an object (Kron 1980). r_{-2} moment is defined as $r_{-2} = [\sum_i (I_i - sky) / \sum_i \{(I_i - sky)/(r_i^2 + 0.5)\}]^{1/2}$.

We have calculated the values of r_{-2} for $r_i \leq 3$ pixels for the detected objects. The range of r_{-2} defined by the obvious bright point sources are derived to be $1.136 < r_{-2}(V) < 1.405$, $1.176 < r_{-2}(I) < 1.465$ for the PC images, and $0.966 < r_{-2}(V) < 1.286$, and $1.027 < r_{-2}(I) < 1.310$ for the WF images. The objects with r_{-2} in these range are classified as point sources. It turns out that most of the objects in the photometry list are extended sources. About 1560

objects among the 5670 detected objects were classified as point sources, and the rest as extended source. These point sources are considered as a final sample of the point sources for the following analysis. Photometry of the bright point sources with $V < 22$ mag are listed in Table 4. Most of these objects are located at $r < 1.1$ arcmin from the center of NGC 4472, and some of them are located out to $r \approx 4$ arcmin (in the N Field and S Field).

3.4. Comparison with Previous Photometry

We have compared our photometry with the Puzia et al.(1999)'s for the globular clusters common between the two studies, as displayed in Fig. 3. Fig. 3 shows that our V and I magnitudes are on average fainter than the Puzia et al.'s, but that the colors agree very well between the two. The mean differences between this study and Puzia et al. are $\Delta V = +0.14 \pm 0.05$ mag for 157 objects with $20 < V < 23$ mag, $\Delta I = +0.15 \pm 0.05$ mag for 176 objects with $19 < I < 22$ mag, and $\Delta(V - I) = -0.01$.

It appears that there are two causes for the photometric differences between the two studies which used the same original *HST* data. First, part of the difference (0.1 mag) is due to the fact that Puzia et al. made a mistake in standard calibration. If the Holtzman zero points that are given for the 0.5 radius arcsec aperture are used, the additional aperture correction of 0.1 mag is not needed to derive the total magnitudes (see Holtzman et al. 1995a,b). However, Puzia et al. applied this correction, making systematically their magnitudes 0.1 mag too bright. Secondly, part of the difference (0.04–0.05 mag) may be due to different methods used in the two studies. We used CCDCAP for the aperture photometry of the point sources in the images where the galaxy light is subtracted, while Puzia et al. used Sextractor (Bertin & Arnouts 1996) for the original images. It is not unexpected that 0.04–0.05 mag difference exists between the different methods of photometry. It is also noted that the scatter in the difference in Fig. 3 is larger than the scatter in the difference among the objects in the overlapped images in our photometry shown in Fig. 2, indicating that the mean errors in our photometry are smaller than the Puzia et al.'s.

Puzia et al. derived also additional aperture corrections for the 0.5 arcsec radius aperture to the infinite radius aperture for the globular clusters, using the modeled light profiles: $C_V = 0.050 \pm 0.015$ mag, $C_I = 0.080 \pm 0.010$ mag, and $C_{(V-I)} = 0.030 \pm 0.018$. Since the modeled light profiles given by Puzia et al. do not match well the bright globular cluster profiles at the outer radius (as shown in their Fig. 1), it is difficult to estimate how reliable the above corrections are. Above comparison of the photometry is based on the Puzia et al.'s photometry before these corrections are applied. If these corrections are included, the magnitude differences between the two studies become larger: $\Delta V = +0.19 \pm 0.05$ mag, $\Delta I = +0.23 \pm 0.05$ mag, and $\Delta(V - I) = +0.01$.

3.5. Artificial Cluster Experiments

We have tested completeness of our photometry using artificial cluster experiment. We have chosen as a test field a field covered by the PC chip for the C1 Field. This PC field includes the nucleus of NGC 4472 in the center of the image so that incompleteness for this field is the most severe among the fields used in this study.

We have derived empirical point spread function of the clusters using several isolated brightest clusters in the images and have created artificial clusters with different magnitudes by scaling down the images of the selected ones. We have created 1000 artificial clusters in 10 images for each filter. Then we have repeated the same reduction procedure to estimate how many objects are recovered from the artificial images. The completeness factors and mean photometric errors obtained in this way are displayed in Fig. 4. Fig. 4 shows that our photometry is complete for $V < 24$ mag, 90% complete at $V \approx 24.6$ mag, and 50% complete at $V \approx 25.2$ mag (at $I \approx 23.6$ mag) for the region at $10 < r < 25$ arcsec. In the innermost region at $r < 10$ arcsec, completeness of our photometry is much lower than the outer region: the completeness is 100% for $V < 23.7$ mag, and 50% at $V \approx 24.5$ mag. The photometry of the other fields must be more complete than this PC field, because the contribution due to varying galaxy light in the other field is much weaker than this PC field.

From this test it is concluded that our photometry is almost complete ($> 95\%$) for $V < 24.2$ mag except for the innermost region at $r < 10$ arcsec. We created a final sample of bright globular clusters with $V < 23.9$ mag used for the analysis of the color of globular clusters, and this sample is considered to be complete. The number of the bright globular clusters with $V < 23.9$ mag in the region at $r < 10$ arcsec is only 11 so that it is negligible compared with the total sample of bright globular clusters used in this study.

4. COLOR-MAGNITUDE DIAGRAM

Figs. 5(a) and 5(b) display the V–$(V-I)$ diagrams of the measured point sources (about 1560 objects) and extended objects (about 4110 objects), respectively. In general, basic features seen in Fig. 5 are similar to those seen in the color-magnitude diagrams of NGC 4472 obtained from the ground-based observations by Geisler et al. (1996), but the HST data go much deeper than the ground-based data. Fig. 5(a) shows a dominant vertical feature at the color range of $0.8 < (V-I) < 1.5$, extending up to $V \approx 19.3$ mag. The objects seen in this feature are mostly globular clusters in NGC 4472. Contamination due to foreground stars is considered to be negligible for this feature. We consider the point sources with $0.75 < (V-I) < 1.45$ as globular cluster candidates from now on. A small number of point sources bluer or redder than this range are probably not the members of NGC 4472.

The vertical structure in the color-magnitude diagram appears obviously to consist of two components: one relatively blue component ($0.75 < (V-I) < 1.08$) and the other relatively red component ($1.08 < (V-I) < 1.45$). We call them, the blue globular clusters (BGCs) and red globular clusters (RGCs), respectively. We create a sample of the bright globular clusters with $V < 23.9$ mag for the detailed analysis of the globular cluster system, considering the photometric errors and the degree of non-member contamination. The boxes in Fig. 5 represent the boundary of these bright globular clusters. The numbers of the blue and red globular clusters with $V < 23.9$ mag are 263 and 346, respectively. The relative abundance of the BGCs and RGCs derived for the inner region of NGC 4472 in this study is opposite to that based on the outer region of NGC 4472 where there are more BGCs than the RGCs (Geisler et al. 1996). These bright globular clusters are a final sample used for the analysis of the colors of the globular clusters later. Fig. 6 displays the positions of the BGCs, RGCs and faint globular cluster candidates with $0.75 < (V-I) < 1.45$ and $23.9 < V < 26$ mag. The property of these two components will be discussed in detail later.

On the other hand, most of the extended objects seen in Fig. 5(b) are fainter than $V \approx 24.5$ mag. These are mostly faint background galaxies, as are often seen in the deep HST images such as the Hubble Deep Field (Williams et al. 1996). The striking difference between the color-magnitude diagram of the point sources and that of the extended sources shows that the image classification used in this study works very well for the HST data. A sharp drop in the number of the extended objects seen at $V < 24.5$ mag in Fig. 5(b) shows that there are few globular clusters candidates among the extended objects, while a large color scatter in the faint magnitudes seen in Fig. 5(a) indicates that there are some contamination due to galaxies in the faint point sources.

We have cross-identified about 190 bright point sources with $18.5 < T_1 < 22.0$ mag common between this study and Geisler et al. (1996). Fig. 4 displays the relation between $(V-I)$ and $(C-T_1)$ colors of these objects. Using the colors and magnitudes of these objects, we have derived transformation relations between VI system and CT_1 system:

$(V-I) = 0.443(C-T_1)+0.396$ for $(C-T_1) < 2.62$ with $\sigma = 0.067$,

$(V-I) = 1.560(C-T_1)-2.533$ for $(C-T_1) > 2.62$ with $\sigma = 0.083$, and

$V = T_1 + 0.110(C-T_1) + 0.024(C-T_1)^2 + 0.444$ with $\sigma = 0.097$.

Fig. 7 shows the color transformation relation obtained in this study in comparison with the relation derived from the photometry of the standard stars by Geisler (1996): $(V-I) = 0.514(C-T_1) + 0.115$ and $V = T_1 + 0.256(C-T_1) + 0.052$. The $(V-I)$ colors derived from the relation obtained in this study is systematically redder than those derived from Geisler's relation (by ~ 0.1 mag for the color of $(C-T_1) = 1.5$ corresponding to the mean color of the globular clusters). We have used the relations derived here for combining the HST VI data in this study with the ground-based CT_1 data (Geisler et al. 1996;Lee et al. 1998) for further analysis.

In this study we adopt the foreground reddening $E(B-V) = 0.0224$ given by Schlegel, Finkbeiner, & Davis (1998), while we adopted a zero foreground reddening given by Burstein & Heiles (1982) in our previous studies (Geisler et al. 1996; Lee et al. 1998). For the extinction to reddening ratio $A_V = 3.1E(B-V)$, corresponding values are $A_V = 0.07$, $A_I = 0.03$, and $E(V-I) = 0.03$.

5. GLOBULAR CLUSTER LUMINOSITY FUNCTION

5.1. Distance Estimate for NGC 4472

We have derived the luminosity functions of the globular clusters (GCLF), which are listed in Table 5 and displayed in Fig. 8. In Fig. 8 the luminosity functions of the total sample look almost Gaussian, with a peak at $V \approx 23.5$ mag.

We have fit a Gaussian function to the data for the range $20.0 < V < 24.4$ mag, for which our photometry is almost complete. We derive the peak luminosities: $V(\max) = 23.50 \pm 0.16$ mag and the width, $\sigma = 1.19 \pm 0.09$, and $I(\max) = 22.40 \pm 0.14$ mag and the width, $\sigma = 1.29 \pm 0.14$. Assuming the peak luminosity of the Galactic globular clusters of $M_V(\max) = -7.4$ mag (Harris 1996;Lee et al. 1998) and the foreground extinction of $A_V = 0.07$ mag, we derive a value for the distance to NGC 4472, $(m - M)_0 = 30.8 \pm 0.2$ and $d = 14.7 \pm 1.3$ Mpc.

We have also compared the luminosity functions in this study with the Puzia et al.'s in Fig. 9. For this comparison we used the same fields as used by Puzia et al., C1, N and S Fields and plotted Puzia et al.'s luminosity functions before incompleteness correction. Also we adjusted the Puzia et al.'s magnitudes by +0.14 mag to match our photometry. Fig. 9 shows that the luminosity functions in the two studies agree well for $V < 23.5$ mag, but that the luminosity function in this study is somewhat higher than Puzia et al.'s for $V > 23.5$ mag, especially for the BGCs. I-band luminosity functions also show similar results, with some deviations for $I > 22.5$ mag. This indicates that our photometry is more complete than Puzia et al.'s before incompleteness correction. We could not compare the luminosity functions after incompleteness correction, because the information given in Puzia et al. is not enough for comparison.

5.2. Comparison of the Peak Luminosity of the BGCs and RGCs

We have investigated whether there is any systematic difference in the peak value of the luminosity functions of the BGCs and RGCs. The V-band luminosity functions of the BGCs and RGCs are also listed in Table 5 and displayed in Fig. 8. Fig. 8 shows that the shapes of the luminosity functions of the two populations are similar and that the peaks are at similar luminosity. From Gaussian fitting to the data, we derive the values for the peak luminosity: $V(\max) = 23.53 \pm 0.16$ mag ($\sigma = 1.16 \pm 0.11$) for the BGCs, $V(\max) = 23.44 \pm 0.22$ mag ($\sigma = 1.16 \pm 0.13$) for the RGCs, $I(\max) = 22.63 \pm 0.26$ mag ($\sigma = 1.24 \pm 0.20$) for the BGCs, and $I(\max) = 22.30 \pm 0.17$ mag ($\sigma = 1.32 \pm 0.21$) for the RGCs. Therefore the peak luminosities of the BGCs and RGCs are similar within the errors. This result is consistent with the results based on the data of the globular clusters in the outer region of NGC 4472 (Lee et al. 1998).

The derived values of the sigma for the two populations are exactly the same for the V-band, and are slightly different for the I-band. If we constrain the sigma as the mean of the two, 1.28, for the I-band, we get $I(\max) = 22.69 \pm 0.13$ mag and 22.37 ± 0.09 mag, respectively, for the BGCs and RGCs. This shows that the difference between the BGCs and RGCs is changed little by constraining the sigma.

The color chosen as the boundary between the BGCs and RGCs, combined with observational errors in color, may affect somewhat the luminosity function that is determined for each group. However, above results are expected to be changed, if any, little, because there is a clear minimum separating between the BGCs and RGCs in the color distribution, and because the total numbers of the clusters in each population are not much different. We performed a Kolmogorov-Smirnov test for the samples derived using the color boundary which is 0.05 mag different from the chosen value. This value of 0.05 mag is five times larger than the mean error of the chosen value. The Kolmogorov-Smirnov test shows that the two populations derived using the color boundary which is 0.05 mag different from the chosen value are the same as the original samples with a probability of 80%. Therefore this effect is found to affect little above results.

On the other hand, Puzia et al. suggested that the peak luminosities of the BGCs are 0.4–0.5 mag brighter than those of the RGCs: $V(\max) = 23.62 \pm 0.09$ mag and $I(\max) = 22.48 \pm 0.07$ for the BGCs, and $V(\max) = 24.13 \pm 0.07$ mag and $I(\max) = 22.90 \pm 0.11$ for the RGCs. If we adjust Puzia et al's magnitudes to match our photometry as shown before, these values will be changed to $V(\max) = 23.76$ mag and $I(\max) = 22.63$ for the BGCs, and $V(\max) = 24.27$ mag and $I(\max) = 23.05$ for the RGCs. Therefore the peak luminosities for the BGCs in this study are similar to the Puzia et al.'s, but the peak luminosities for the RGCs in this study as much as 0.8 mag brighter than the Puzia et al.'s.

The causes for this large difference for the RGCs

between the two studies are not clear. However, there are a few reasons that our results are considered to be more reliable than the Puzia et al.'s. First, the peak luminosity differences between the BGCs and RGCs given by Puzia et al. are significantly different between the C1 Field and (N+S) Fields: $\Delta V = -0.42$ mag and $\Delta I = -0.21$ mag for the C1 Field, and $\Delta V = -0.68$ mag and $\Delta I = -0.64$ mag for the (N+S) Fields. This indicates that there may be some problems in the data even after the incompleteness correction of their sample. Secondly, our sample of globular clusters is about 30% larger than Puzia et al.'s (because we included the C2 field which was not used by Puzia et al.). Thirdly, our photometry is more complete than Puzia et al.'s.

Puzia et al. used further these differences in magnitudes between the BGCs and RGCs to investigate any age differences between the two components. From the comparison of the peak luminosities of the BGCs and RGCs with the simple stellar population models (Worthey 1994; Bruzual and Charlot 1996; Maraston 1998; Kurth et al 1999) Puzia et al. concluded that $0.4 - 0.5$ mag differences between the two components indicate that the BGCs and RGCs are coeval within the errors of ~ 3 Gyrs. However, our results indicate that the RGCs are several Gyrs younger than the BGC, if we use the same models used by Puzia et al. (their Figures 9, 10, 11 and 12).

Our result on the age difference is similar to the results for the globular clusters in the inner region of M87 (Kundu et al. 1999). Kundu et al. (1999) found from the analysis of the WFPC images of the inner region of M87 that the BGCs are 0.2–0.3 mag brighter than the RGCs at V-band, and that the RGCs are 0.06 mag brighter than the BGCs at I-band, and suggested that the RGCs may be 3–6 Gyrs younger than the BGCs.

5.3. Spatial Variation of the Luminosity Function

Globular clusters in the inner region of giant galaxies are ideal targets to study the dynamical effects on the globular cluster system due to external processes. Primary external processes driving dynamical evolution of globular clusters are tidal shocks and dynamical friction. According to the theoretical prediction, the most massive clusters will be preferentially depleted by dynamical friction, while less massive clusters with lower density will be more efficiently destroyed by tidal shocks. These external dynamical effects are expected to be strongly enhanced in the inner region of the galaxies (Ostriker & Gnedin 1997;Gnedin 1997;Murali & Weinberg 1997a,b,c). As results of these effects, it is expected that the globular cluster luminosity function for the inner region of a galaxy will get flatter than that for the outer region, and the peak luminosity for the inner region will get brighter than that for the outer region. However, several observational studies found little evidence supporting these theoretical predictions in the case of the globular clusters of M87 (Harris et al. 1998;Kundu et al. 1999).

NGC 4472 is another good galaxy to study this aspect. We have investigated whether the globular cluster luminosity function of NGC 4472 shows any systematic variation on the galactocentric distance, using three methods: a) the slope of the bright globular cluster luminosity function, b) the peak luminosity of the globular cluster luminosity function, and c) the mean luminosity of the bright globular clusters. Fig. 10 displays the globular cluster luminosity function for five radial bins. We have fit the data for the bright part in the range of $21.5 < V < 23.5$ mag using a logarithmic line to check any systematic variation in the slope, the results of which are shown by the dashed line. There is seen little systematic variation depending on the galactocentric radius in the logarithmic slope of the bright part of the luminosity function. Next we display the peak luminosity of the V and I bands globular cluster luminosity function for each radial bin in Fig. 11. Fig. 11 shows little systematic variation of the peak luminosity depending on the galactocentric radius within $r = 2.5$ arcmin. The peak luminosity at the outermost position of $r = 3.3$ arcmin seems to be 0.3 mag fainter than the mean value shown by the dashed line in Fig. 11. This may be either an intrinsic property of the globular clusters or may be caused by the fact that the degree of field contamination due to background galaxies is increasing in the outer region (see the asymmetric globular cluster luminosity function for $2'.67 < r < 4'.00$ in Fig. 10). This point needs to be checked with similar HST observations for larger areas in NGC 4472. However, the following result indicates that the first possibility is low.

We have calculated the mean luminosity of the bright globular clusters with $20 < V < 23.5$ mag. The magnitude range is chosen that the resulting mean luminosity is not affected at all by incompleteness in our photometry. Fig. 12 displays the mean luminosity

of the globular clusters versus galactocentric radius based on the HST data, and Table 6 lists the linear fits to the data. Fig. 12 shows that there is little, if any, change in the mean luminosity of the bright globular clusters for the region at $r < 4$ arcmin from the center of NGC 4472 (the determined values of the slope are smaller than the errors). This result is similar to that of the globular clusters in the inner region of M87 (Harris et al. 1998;Kundu et al. 1999).

Then we have combined these HST data with those for the outer region of NGC 4472 given by Geisler et al. (1996) to investigate any gradient of the mean luminosity over a large range of radius, the results of which are illustrated in Fig. 13. Fig. 13 shows that the mean luminosity of the BGCs is clearly decreasing by about 0.2 mag over the range of $r = 9$ arcmin (the slope $= 0.024 \pm 0.010$ for V and I), while the mean luminosity of the RGCs is almost constant over the same range of radius. This result of the difference between the BGCs and RGCs is not affected by the errors involved with combining the HST data and the ground-based data, because it is based on the globular clusters with the same magnitude range.

Therefore it is concluded that there is little systematic variation of the globular cluster luminosity function within the range of $r = 4$ arcmin, and that the BGCs on average become fainter by 0.2 mag with the increasing galactocentric radius over the range of 9 arcmin, while the RGCs do not. This result shows that the external dynamical effects are much weaker than the theoretical predictions for the globular cluster systems in NGC 4472. The cause for the 0.2 mag variation of the mean luminosity seen only for the bright BGCs is unclear. If it is due to dynamical effects, it may indicate that the BGCs are older than the RGCs.

6. GLOBULAR CLUSTER COLOR DISTRIBUTION

We have derived a color distribution of the bright globular clusters with $V < 23.9$ mag in NGC 4472, which is listed in Table 7 and displayed in Fig. 14. Fig. 14 shows that the color distribution of the globular clusters is clearly bimodal. From double-Gaussian fitting to the data, we have derived the peak colors $(V - I) = 0.975 \pm 0.005$ with $\sigma = 0.076$, and $(V - I) = 1.233 \pm 0.006$ with $\sigma = 0.094$. These results agree very well with those given for $V < 23.75$ mag by Puzia et al. (1999): $(V - I) = 0.99 \pm 0.01$ and 1.24 ± 0.01, respectively.

Using the relation between $(V - I)$ and metallicity of Galactic globular clusters given by Kundu & Whitmore (1998), $[\mathrm{Fe/H}] = -5.89 + 4.72(V - I)$, and adopting the reddening of $E(V - I) = 0.03$, we derive the peak metallicities [Fe/H] $= -1.41$ and –0.23 dex for the BGCs and RGCs, respectively, from the peak colors. (If we use the slightly different relation used by Harris et al. (1998), $[\mathrm{Fe/H}] = -6.67 + 5.56(V - I)$, we derive [Fe/H] $= -1.39$ and $+0.00$ dex for the BGCs and RGCs, respectively.) The mean color of the bright globular clusters with $V < 23.9$ mag is derived to be $(V - I) = 1.11 \pm 0.01$ (m.e.), corresponding to the metallicity of [Fe/H] $= -0.79 \pm 0.05$ dex. These results for the peak metallicity are in good agreement with the results for the globular clusters in the outer region of NGC 4472 (Geisler et al. 1996; Lee et al. 1998).

However, the relative abundance of the BGCs and RGCs is opposite between the inner region (this study) and the outer region (Geisler et al. 1996). In the inner region, the RGCs are more numerous than the BGCs, while it is opposite in the outer region. Fig. 15 displays a radial variation of the color distribution of the bright globular clusters. It shows that the relative number of the BGCs to that of the RGCs is increasing as the galactocentric distance is increasing.

In Fig. 16 we display a radial variation of the number of the BGCs to that of the RGCs (= N(BGC)/N(RGC)). We also plot the data of the globular clusters with $T_1 < 23$ mag in the outer region of NGC 4472 derived from Geisler et al. (1996). Fig. 16 shows that the radial variation of the ratio is consistent between the inner region and the outer region. The ratio N(BGC)/N(RGC) increases continuously out to the limit of the data, ~ 9 arcmin.

7. SPATIAL STRUCTURE OF THE GLOBULAR CLUSTER SYSTEM

We have investigated the spatial structure of the globular cluster system in NGC 4472 using the sample of the bright globular clusters with $V < 23.9$ mag. Without the HST data it is very difficult to study the spatial structure of the globular cluster systems in the central region of NGC 4472. Fig. 17 displays the spatial positions of these objects in the central 2.4×2.4 arcmin^2 region of NGC 4472. It is seen immediately in Fig. 17 that the RGCs are more centrally concen-

trated than the BGCs. Radial and azimuthal structures of the globular cluster system are studied in the following.

7.1. Radial Structure

7.1.1. Surface Number Density

We have derived radial profiles of the surface number density of the globular clusters with $V < 23.9$ mag, which are listed in Table 8 and are displayed in Fig. 18. Fig. 18 shows (a) that the surface density increase with decreasing radius, (b) that the surface density profiles of both the RGCs and BGCs get flat in the central region, and (c) that the surface density profile of the RGCs is steeper than that of the BGCs.

The surface density profiles within $r \sim 2$ arcmin are approximately fit by King models(King 1966): core radius $r_c = 1.3$ arcmin (= 6.0 kpc), concentration parameter $c = \log(r_t/r_c) = 3.0$ (where r_t is a tidal radius), and peak surface density $\sigma_{GC}(0) = 81.3$ clusters arcmin^{-2} for the total sample, $r_c = 1.9$ arcmin (= 8.7 kpc), $c = 2.25$, and $\sigma_{GC}(0) = 26.0$ clusters arcmin^{-2} for the BGCs, and $r_c = 1.2$ arcmin (= 5.5 kpc), $c = 2.25$, and $\sigma_{GC}(0) = 51.3$ clusters arcmin^{-2} for the RGCs. The core radius of the globular cluster system derived here is much larger than that of the stellar halo, $r_c = 3.6$ arcsec (= 280 pc) given by Kim, Lee & Geisler (2000).

In Fig. 19 we display both the surface density profiles for the globular clusters in the inner region derived in this study and those for the globular clusters with $T_1 < 23.0$ mag in the outer region given by Lee et al. (1998). The lower limit for the outer globular cluster sample, $T_1 = 23.0$ mag, corresponds to $V \approx 23.7$ mag for the mean color of the globular clusters. We plot the surface density profile of the inner globular clusters with $V < 23.7$ mag in Fig. 19. Note that the surface density profiles of both data agree approximately for the overlapped region at $1 < r < 3$ arcmin. The surface density profiles of the combined data of the outer region at $r > 55$ arcsec are well fit by de Vaucouleurs law:

$\log \sigma_{GC} = -1.318(\pm 0.048) r^{1/4} + 2.905(\pm 0.062)$ for the total sample,

$\log \sigma_{GC} = -0.890(\pm 0.058) r^{1/4} + 2.087(\pm 0.076)$ for the BGCs, and

$\log \sigma_{GC} = -1.778(\pm 0.063) r^{1/4} + 3.148(\pm 0.080)$ for the RGCs,

where r is given in units of arcmin.

7.1.2. Color

We have derived the radial profiles of the mean and median color of the globular clusters, which are listed in Table 9 and displayed in Fig. 20. We also displayed the radial profile of the color of the halo of NGC 4472 in Fig. 20 to compare the globular clusters and halo of NGC 4472. We have transformed the $(C - T_1)$ color of the halo of NGC 4472 (Kim, Lee & Geisler 2000) into the $(V - I)$ color using the relation derived in this study. Fig. 20 shows (a) that the mean color of the total sample of globular clusters decreases with increasing radius for $r > 1$ arcmin, (b) that the mean colors of the BGCs and RGCs change little with increasing radius, and (c) that the profile of the RGCs is very similar to that of the halo. These results are consistent with those for the outer region given in Lee et al. (1998).

Fig. 21 shows the radial profiles of the metallicity of the globular clusters derived from the colors based on this study (filled circles) and Geisler et al. (1996) (open circles). The mean metallicity is increasing with decreasing galactocentric radius. However, the metallicity becomes almost constant within $r \sim 1$ arcmin, where the surface number density of the globular clusters is almost constant as shown in Fig. 18.

Interestingly Harris et al. (1998) also pointed out a similar trend from the ground-based data for M87: the mean metallicity of the globular clusters in M87 is almost constant for $r < 1$ arcmin. However, Kundu et al. (1999) mentioned that their observations of the inner region of M87 based on the *HST* data do not provide any compelling supporting evidence for the claim by Harris et al. (1998).

The metallicity profile for the combined sample of the inner region and outer region ($r > 50$ arcsec) is fit by [Fe/H]$= -0.390(\pm 0.054) \log r + 0.120(\pm 0.124)$ with $\sigma = 0.037$, where r is given in terms of arcmin. This result is very similar to that derived for the outer region, shown by the dashed line with a slope of –0.41 in Fig. 21 (Geisler et al. 1996).

7.2. Azimuthal Structure

We have investigated the azimuthal distribution of the globular clusters. Fig. 22 displays azimuthal variations of the globular cluster number density for $r < 1.1$ arcmin where the areal coverage of the *HST* data is complete. It shows that the total sample has obvious peaks at a position angle of 160 and 340 deg and that the RGCs have a peak at 160 deg, while

the BGCs show an almost uniform distribution. The presence of only one peak instead of two for the RGCs is due to the asymmetric distribution of the globular clusters extended along the south-east direction, as shown in Fig. 17.

8. DISCUSSION

8.1. Comparison of the Globular Clusters in the Inner and Outer Regions of NGC 4472

In this study we have investigated several aspects of the globular clusters in the inner region of NGC 4472: color-magnitude diagram, luminosity function, color distribution, and spatial structure of the globular cluster system. *HST* data enable us to study the globular clusters located close to the nucleus of NGC 4472, which was difficult in the case of ground-based data.

We have compared these results to those of the globular clusters in the outer region of NGC 4472 (Geisler et al. 1996;Lee et al. 1998), finding that the properties of the globular clusters in the inner region and the outer region of NGC 4472 are in general similar. The only exception is that there are more RGCs than the BGCs in the inner region, while it is opposite in the outer region. However, this is also expected from the relation of N(BGC)/N(RGC) and galactocentric distance derived from the data of the outer region.

Implications of the results based on the globular clusters in the outer region of NGC 4472 for the origin of the globular clusters were discussed in detail in Lee et al. (1998), which remain still valid with the new results for the globular clusters in the inner region of NGC 4472. In summary, the observed properties are consistent with many of the predictions of both the model of episodic in situ formation plus tidal stripping of globular clusters given by Forbes, Brodie & Grillmair (1997), and the gaseous merger model given by Ashman & Zepf (1992), but each of the models also has some problems.

8.2. Comparison of the Globular Clusters in the Inner Regions of NGC 4472 and M87

NGC 4472 and M87 (NGC 4486) are the two most dominant galaxies in the Virgo cluster. NGC 4472 is the brightest member of the Virgo cluster, but not a cD galaxy, while M87 is a cD galaxy at the center of the Virgo cluster and is only slightly fainter than NGC 4472. M87 has been a target of much more studies than NGC 4472. Recently Kundu et al. (1999) presented a study of 1057 globular clusters in the inner region ($r < 1.5$ arcmin) based on the *HST* WFPC2 data of a field centered on the nucleus of M87. The areal coverage of their data is similar to that of C1 and C2 Fields in our study. Kundu et al. adopted foreground extinctions of $A_V = 0.067 \pm 0.04$ and $A_I = 0.032 \pm 0.02$ in their study of M87, which are the same adopted for NGC 4472 in this study. We have compared the properties of the globular clusters in the inner region of these two galaxies based on the similar data (this study and Kundu et al. 1999).

The luminosity function of the M87 globular clusters has a peak at $V_0(\max) = 23.67 \pm 0.07$ mag with $\sigma = 1.39 \pm 0.06$, which are slightly larger than that of NGC 4472, $V_0(\max) = 23.43 \pm 0.08$ mag with $\sigma = 1.19 \pm 0.09$. Thus NGC 4472 is considered to be slightly closer than M87. The luminosity function of the M87 globular clusters does not show any significant spatial variation over the radius of 1.5 arcmin, similarly to the case of NGC 4472.

The color distribution of the globular clusters in M87 is also bimodal. The peak colors are $(V-I)_0 = 0.95$ and 1.20 and the mean color of the total sample is $(V-I)_0 = 1.09$. These values are essentially the same as those of the globular clusters in NGC 4472, $(V-I)_0 = 0.95$, 1.20 and 1.08. Thus the characteristic colors of the globular clusters in NGC 4472 and M87 are almost the same.

The surface number density profiles of the globular clusters are flat in the central regions of both M87 and NGC 4472. The core radii of the globular clusters in the inner region of M87 and the stellar halo are, respectively, 56 arcsec and 6.8 arcsec (Kundu et al. 1999). Therefore the core of the globular cluster system in M87 is somewhat smaller than that of NGC 4472, 78 arcsec, while the core of the stellar halo in M87 is twice larger than that of NGC 4472, 3.6 arcsec. The relative number of the BGCs to that of the RGCs in M87 is also increasing with increasing galactocentric radius, as in the case of NGC 4472. The absence of the spatial variation of the globular cluster luminosity function and the core radius of the globular cluster systems larger than the stellar core of the galaxies are considered to support the suggestion that the large core of the globular cluster systems is a relic of the cluster formation process rather than a result due to destruction through tidal shock-

ing and dynamical friction (Grillmair, Pritchet, & van den Bergh 1986, Harris et al. 1998).

However, the surface central number density of the globular clusters is about six times larger in M87 (460 clusters arcmin^{-2}) than in NGC 4472 (81 clusters arcmin^{-2}). This indicates that the conditions of formation process of globular clusters might have been different between M87 and NGC 4472.

In summary, we conclude that the properties of the globular clusters in the inner regions of NGC 4472 and M87 are very similar in general. The only significant difference is that the surface central number density of the globular clusters (and the specific frequency of the globular clusters correspondingly) is much higher in M87 than in NGC 4472.

9. SUMMARY AND CONCLUSION

We have presented VI photometry of the globular cluster candidates in the inner ($r < 4$ arcmin) region of NGC 4472, derived from the *HST* WFPC2 archive data for the four fields of NGC 4472. We have found about 1560 globular cluster candidates from the colors and image classifiers. Primary results and conclusions obtained in this study are summarized as follows.

1. The color-magnitude diagram of the measured point sources shows a dominant vertical structure at the color range of $0.75 < (V-I) < 1.45$, most of which are globular clusters in NGC 4472. This structure consists obviously of two populations: the blue globular clusters and the red globular clusters.

2. The luminosity function of the globular clusters is well fit by a Gaussian function with a peak at $V = 23.50 \pm 0.16$ mag and $\sigma = 1.19 \pm 0.09$. From this the distance to NGC 4472 is derived to be $d = 14.7 \pm 1.3$ Mpc. The globular cluster luminosity function shows little systematic variation depending on the galactocentric radius. There is little difference in the peak luminosity between the BGCs and RGCs. This indicates that the RGCs may be several Gyrs younger than the BGCs, contrary to the conclusion given by Puzia et al. (1999).

3. The color distribution of the 609 bright globular clusters with $V < 23.9$ mag is distinctively bimodal with peaks at $(V-I) = 0.975$ and 1.233. The metallicities corresponding to these peaks are [Fe/H] $= -1.41$ and -0.23 dex. The mean color of the bright globular clusters with $V < 23.9$ mag is derived to be $(V-I) = 1.11 \pm 0.01$(m.e.), corresponding to the metallicity of [Fe/H] $= -0.79 \pm 0.05$ dex.

4. The ratio of the number of the BGCs to that of the RGCs is increasing with increasing galactocentric radius from the center out to about 9 arcmin. Thus the RGCs are more centrally concentrated than the BGCs.

5. The surface number density profile of the globular clusters in the inner region is approximately fit by a King model with core radius $r_c = 1.3$ arcmin, while that of the globular clusters in the outer region is better fit by de Vaucouleurs law. The core radius of the globular cluster system obtained in this study is much larger than that of the stellar halo.

6. The mean colors of the BGCs and RGCs change little with increasing radius, and the mean color of the RGCs is very similar to that of the stellar halo of NGC 4472.

7. The radial gradient of the metallicity of the entire sample of the globular clusters with $V < 23.9$ mag is approximately fit by [Fe/H] $= -0.390 \log r + 0.120$ with $\sigma = 0.037$, where r is given in the unit of arcmin.

8. In general the property of the globular clusters in the inner region of NGC 4472 is consistent with that of the globular clusters in the outer region of NGC 4472, except that there are more RGCs than the BGCs in the inner region.

The authors are grateful to Sang Chul Kim for careful reading of the manuscript of this paper and to Thomas Puzia for providing the photometry data of the globular clusters of NGC 4472 used in Puzia et al. (1999) and useful information. Anonymous referee is thanked for useful comments. This research is supported in part by the KOSEF/KISTEP International Collaboration Research Program (1-99-009).

REFERENCES

Ashman, K.M., & Zepf, S. E. 1992, ApJ, 384, 50

Bertin, E., & Arnouts, S. 1996, A&AS, 117, 393

Bruzual, A. G., & Charlot, S. 1996, electronically available. See Leitherer, C., et al. 1996, PASP, 108, 996

Burstein, D., & Heiles, C. 1982, AJ, 87, 65

Forbes, D. A., Brodie, J. P., & Grillmair, C. J. 1997, AJ, 113, 1652

Gebhardt, K., & Kissler-Patig, M. 1999, ApJ, 118, 1526

Geisler, D. 1996, PASP, 111, 480

Geisler, D., Lee, M. G., & Kim, E. 1996, AJ, 111, 1529

Gnedin, O. Y. 1997, ApJ, 487, 663

Grillmair, C. J., Pritchet, C., & van den Bergh, S. 1986, AJ, 91, 1328

Harris, W. E. 1996, AJ, 112, 1487

Harris, W. E., Harris, G. L. H., & McLaughlin, D. E. 1998, ApJ, 115, 1801

Holtzman, J. et al. (the WFPC2 team) 1995a, PASP, 107, 156

Holtzman, J. et al. (the WFPC2 team) 1995b, PASP, 107, 1065

Kim, E., Lee, M. G., & Geisler, D. 2000, MNRAS, in press

King, I. 1966, AJ, 71, 276

Kron, R. 1980, ApJS, 43, 305

Kundu, A. 1999, Ph.D. Thesis, University of Maryland

Kundu, A., Whitmore, B. C. 1998, AJ, 116, 2841

Kundu, A., Whitmore, B. C., Sparks, W. B., Macchetto, F. D., Zepf, S. E., & Ashman, K. M. 1999, ApJ, 513, 733

Kurth, O. M., Fritze-v. Alvensleben, U., & Fricke, K. J. 1999, A&AS, 138, 19

Lee, M. G., Kim, E. & Geisler, D. 1998, AJ, 115, 947

Maraston, C. 1998, MNRAS, 300, 872

Mighell, K. 1998, private communication

Murali, C., & Weinberg, M. D. 1997a, MNRAS, 288, 749

Murali, C., & Weinberg, M. D. 1997b, MNRAS, 288, 767

Murali, C., & Weinberg, M. D. 1997c, MNRAS, 291, 717

Ostriker, J. P., & Gnedin, O. Y. 1997, ApJ, 487, 667

Puzia, T. H., Kissler-Patig, M., Brodie, J. P., & Huchra, J. P. 1999, AJ, 118, 2734

Schlegel, D. J., Finkbeiner, D. P., & Davis, M. 1998, ApJ, 500, 525

Williams, R. et al. 1996, AJ, 112, 1335

Worthey, G. 1994, ApJS, 95, 107

This 2-column preprint was prepared with the AAS LaTeX macros v4.0.

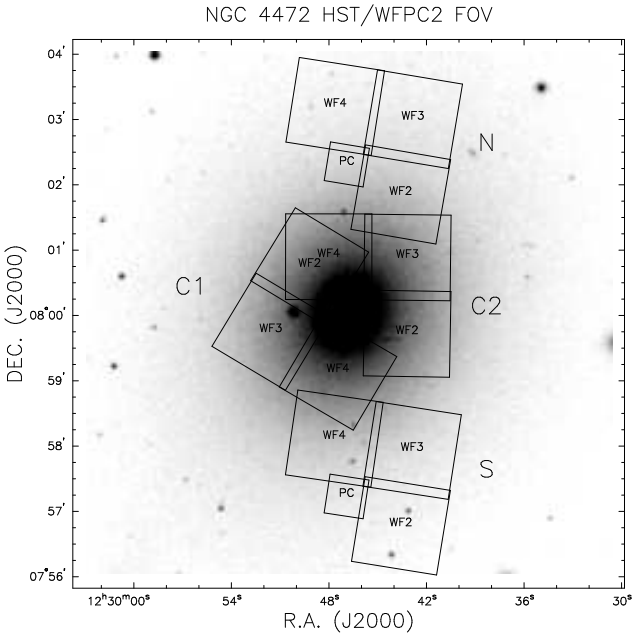

Fig. 1.— Digitized Sky Survey image of the region showing positions and orientations of the *HST*/WFPC2 fields of NGC 4472.

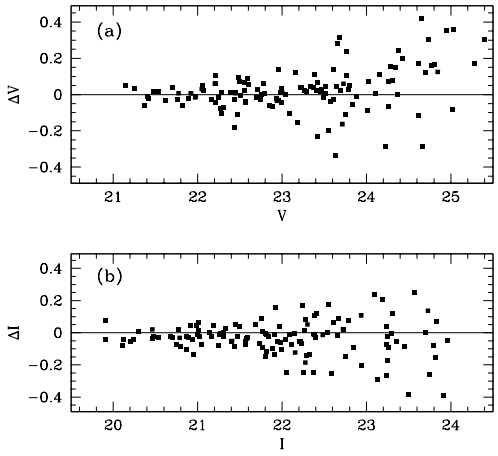

Fig. 2.— Comparison of the photometry of the objects common in overlapped regions between neighboring fields for V (a) and I (b).

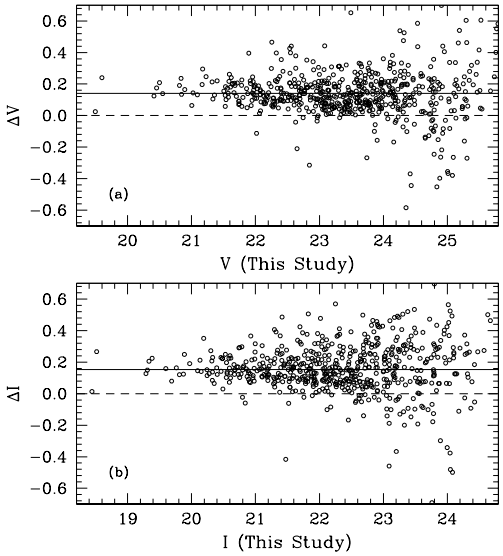

Fig. 3.— Comparison of the photometry of the objects common in this study and Puzia et al.(1999). The differences are given in terms of this study minus Puzia et al.'s. The solid lines represent the median value of the differences.

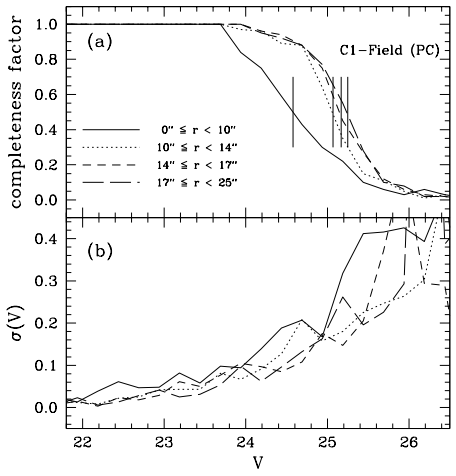

Fig. 4.— (a) Completeness of our photometry for the PC chip of the C1 Field, the center of which corresponds almost the center of NGC 4472. Therefore the incompleteness is expected to be the highest among the fields used in this study. Different types of lines represent the regions at different radius from the center of NGC 4472. The vertical bars represent the level of 50% completeness. (b) Mean photometric errors versus magnitudes obtained from the artificial object experiment.

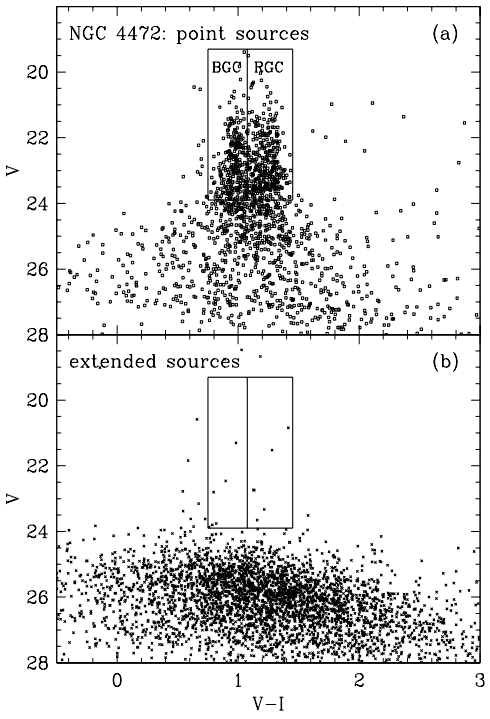

Fig. 5.— (a) V vs. $(V-I)$ diagram of the measured point sources in the images of NGC 4472. The boundaries for the blue globular clusters (BGCs) and red globular clusters (RGCs) brighter than $V = 23.9$ mag are marked by the boxes. (b) V vs. $(V-I)$ diagram of the measured extended sources in the images of NGC 4472.

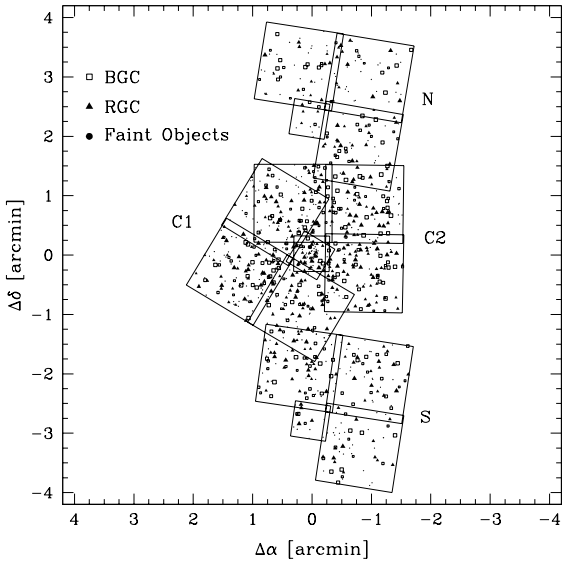

Fig. 6.— Positions of the globular cluster samples. Open squares, filled triangles and dots represent, respectively, the BGC with $V < 23.9$ mag, RGC with $V < 23.9$ mag and faint globular clusters with $23.9 < V < 26$ mag.

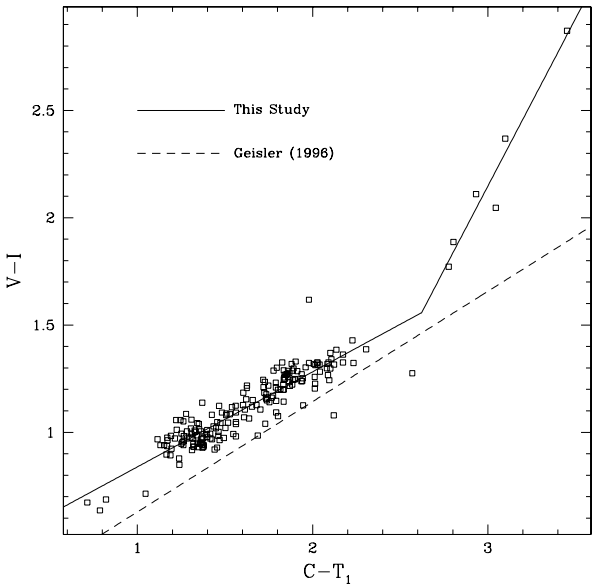

Fig. 7.— $(V - I)$ vs. $(C - T_1)$ of the point sources in NGC 4472 common between this study and Geisler et al. (1996). The solid line represents double-linear fits to the data and the dashed line represents a transformation relation given by Geisler (1996).

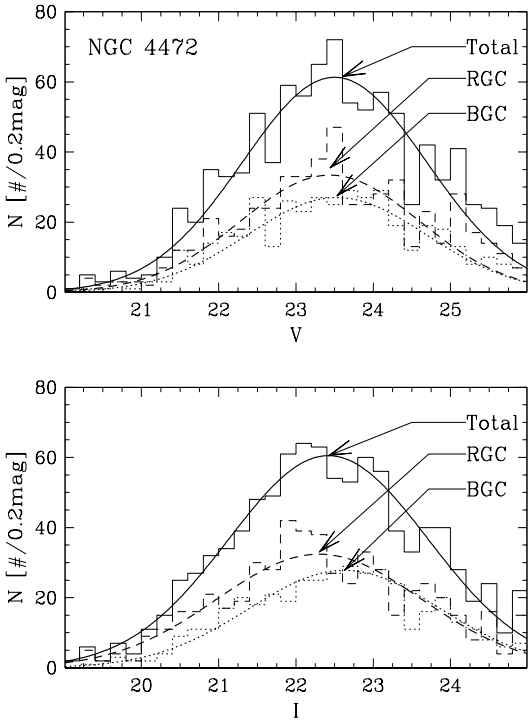

Fig. 8.— V-band and I-band luminosity functions of the globular cluster candidates in NGC 4472 (histograms). The solid line, dashed line, and dotted lines represent, respectively, the luminosity functions for the total sample, RGCs, and BGCs. The curved lines show Gaussian fits to the data.

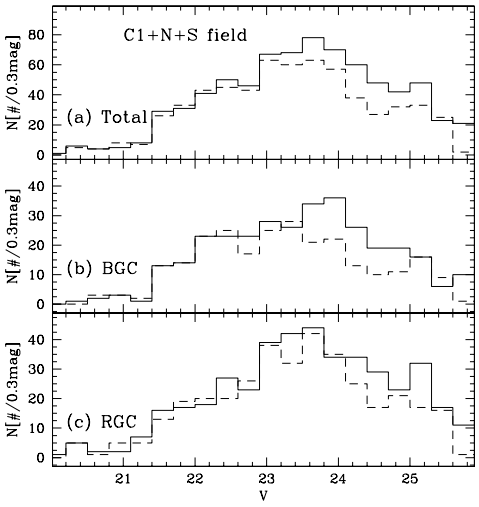

Fig. 9.— Comparison of the globular cluster luminosity functions (before incompleteness correction) of this study (the solid line) and Puzia et al. (1999) (the dashed line). For the purpose of comparison, only C1, N and S fields are used to derive the luminosity functions, as used by the latter. Same color ranges are used for both samples: $0.75 < (V-I) < 1.08$ for the blue globular clusters and $1.08 < (V-I) < 1.45$ for the red globular clusters. V magnitudes of Puzia et al.'s are adjusted by +0.14 mag to match our photometry. Note that there are somewhat more objects at $V > 23.5$ mag in this study than in Puzia et al., showing that our sample is more complete than the latter.

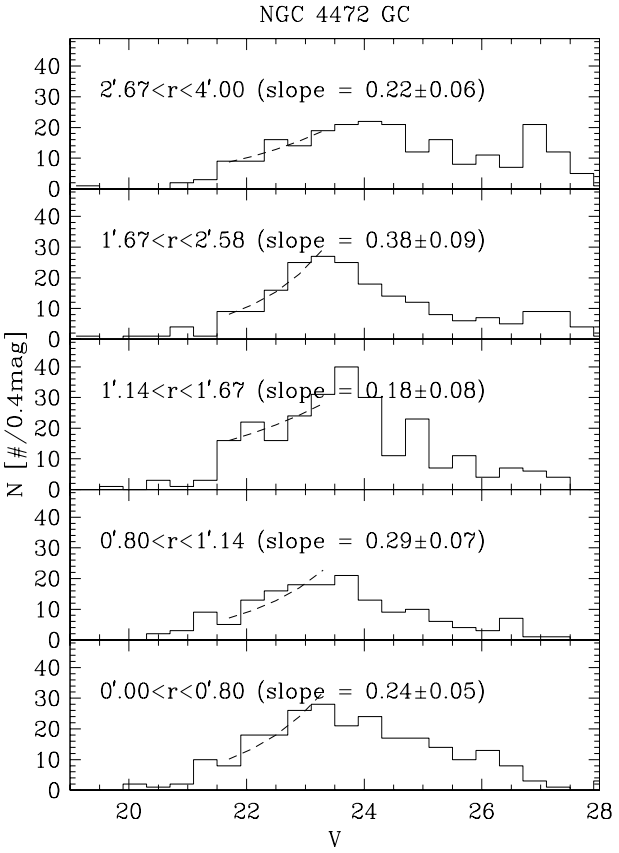

Fig. 10.— Radial variation of the globular cluster luminosity function for NGC 4472. The dashed lines represent logarithmic fits to the data for the range of $21.5 < V < 23.5$ mag. Note that there is little systematic change in the slope of the fitted data as the galactocentric distance changes.

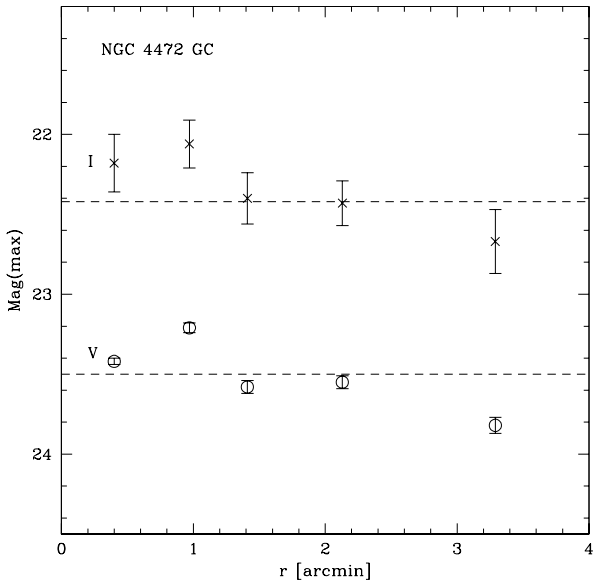

Fig. 11.— Radial variation of the peak luminosity of the globular cluster luminosity functions for V and I bands. The dashed lines represent the peak luminosity of the entire sample.

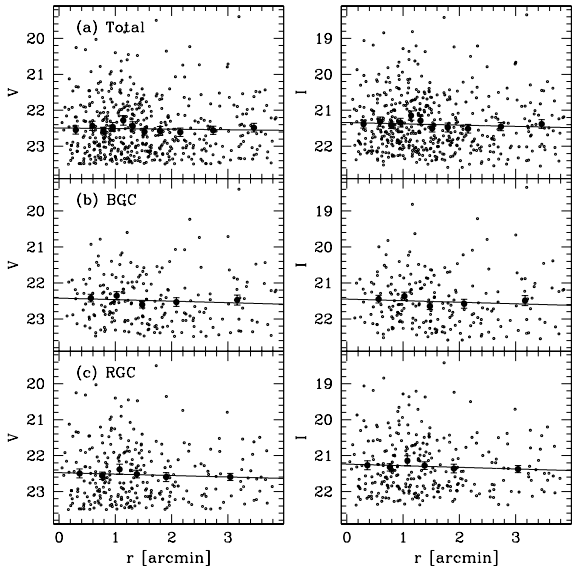

Fig. 12.— Radial variation of the mean magnitude of the bright globular clusters with $V < 23.5$ mag in the HST sample (the filled circles). The solid lines represent linear fits to the mean magnitudes. Note that there is little change in the mean magnitude with increasing galactocentric distance.

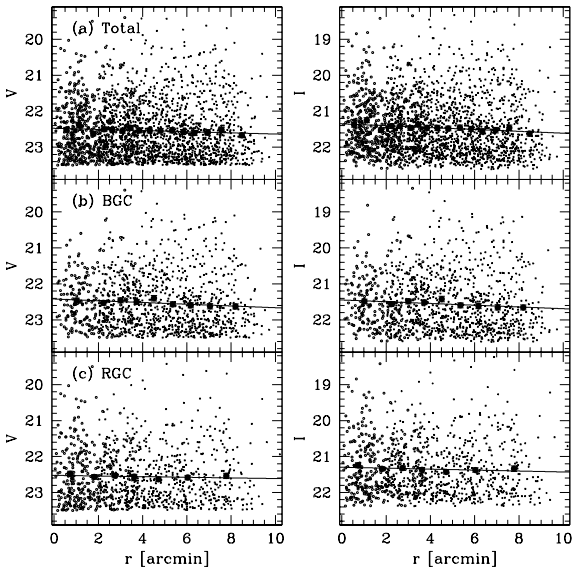

Fig. 13.— Radial variation of the mean magnitude of the bright globular clusters with $V < 23.5$ mag in the HST sample (the open circles) and the ground-based sample given by Lee et al. (1998) (the crosses). The solid lines represent linear fits to the mean magnitudes.

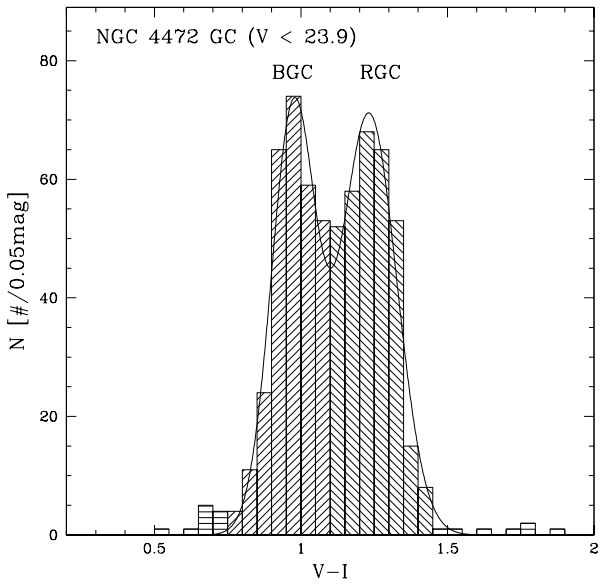

Fig. 14.— Color distribution of the bright globular clusters with $V < 23.9$ mag in NGC 4472. The curved lines show double-Gaussian fits to the data .

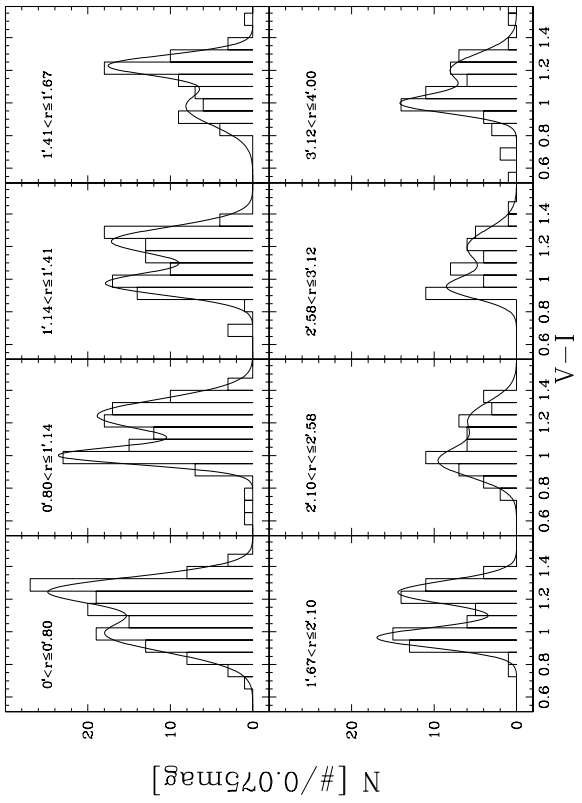

Fig. 15.— Radial variation of the color distribution of the globular clusters with $V < 23.9$ mag in NGC 4472. The curved lines show double-Gaussian fits to the data.

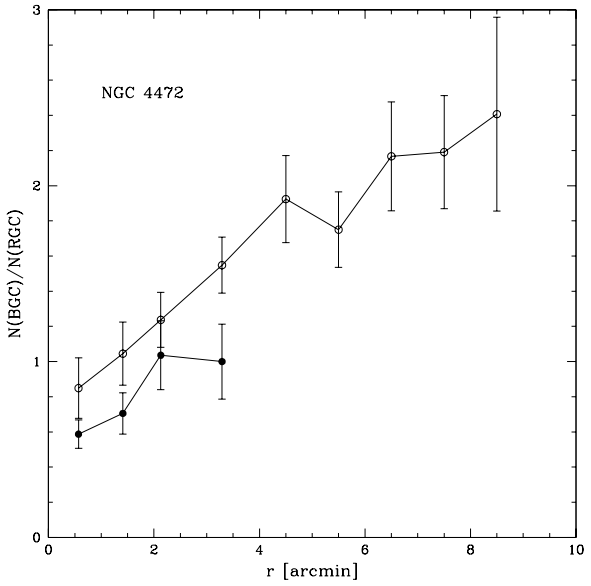

Fig. 16.— Radial variation of the number of the BGCs to that of the RGCs with $V < 23.9$ mag in NGC 4472 (filled circles). The open circles represent the data for the globular clusters with $T_1 < 23$ mag in the outer region of NGC 4472 derived from Geisler et al. (1996).

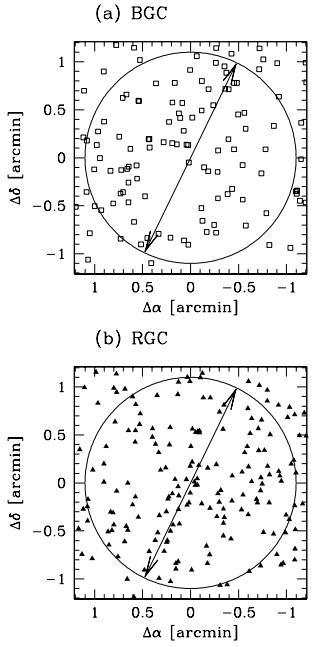

Fig. 17.— Spatial distribution of the blue (a) and red (b) globular clusters brighter than $V = 23.9$ mag in the central region of NGC 4472. The radius of the circle is 1.1 arcmin and the arrow represents the direction of the major axis of the stellar halo.

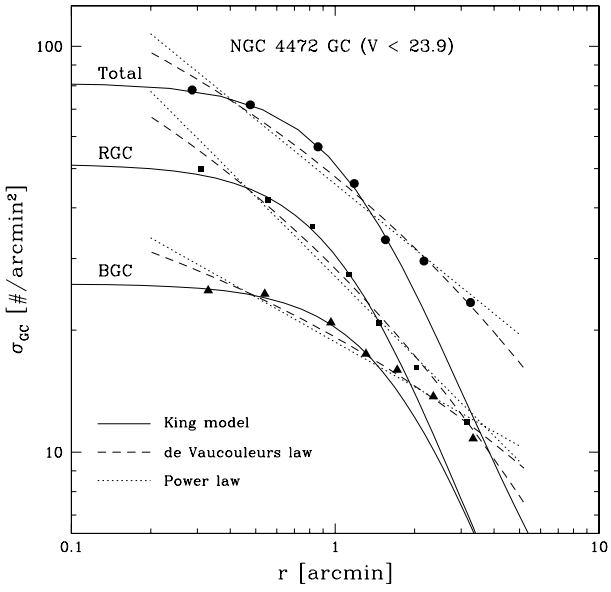

Fig. 18.— Radial variation of the surface number density of the bright globular clusters with $V < 23.9$ mag in the inner region of NGC 4472. The circles, triangles, and squares represent, respectively, the total sample, blue globular clusters, and red globular clusters. The solid line, dashed line and dotted line show, respectively, fits to the data with King model, de Vaucouleurs law and power law.

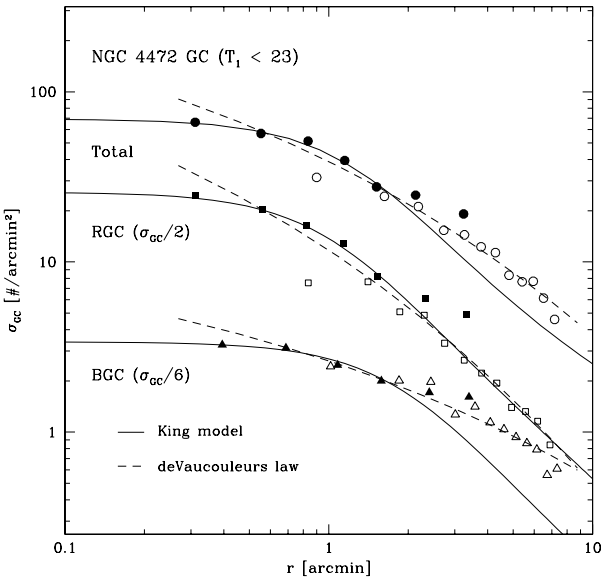

Fig. 19.— Radial variation of the surface number density of the bright globular clusters in the inner region ($V < 23.7$ mag corresponding to $T_1 < 23.0$ mag, filled symbols) and the outer region ($T_1 < 23.0$ mag, open symbols) of NGC 4472 given by this study and Lee et al. (1998). The circles, triangles, and squares represent, respectively, the total sample, blue globular clusters, and red globular clusters. The solid line and dashed line show, respectively, fits to the data with King model and de Vaucouleurs law. The data for the RGCs and BGCs were scaled down, respectively, by a factor of 1/2 and 1/6 to show the data better.

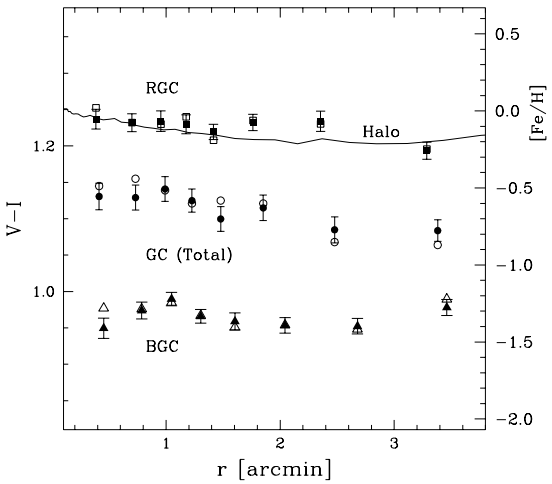

Fig. 20.— Radial variation of the mean (filled symbols) and median (open symbols) color of the bright globular clusters with $V < 23.9$ mag in NGC 4472. The circles, triangles, and squares represent, respectively, the total sample, blue globular clusters, and red globular clusters. The solid line represents the mean color of the stellar halo of NGC 4472 given by Kim, Lee & Geisler (2000).

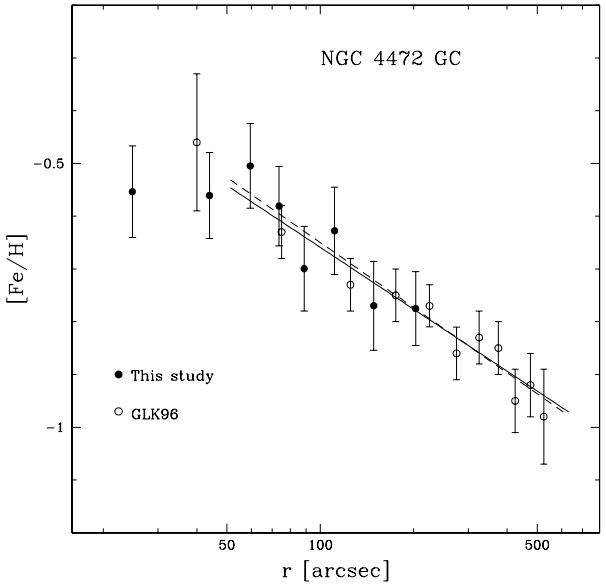

Fig. 21.— Radial variation of the mean metallicity of the bright globular clusters in the wide region of NGC 4472. The filled and open circles represent, respectively, the data in this study and those given by Geisler et al. (1996). The solid line shows a linear fit to the combined data of two studies, and the dashed line represents a linear fit given by Geisler et al. (1996).

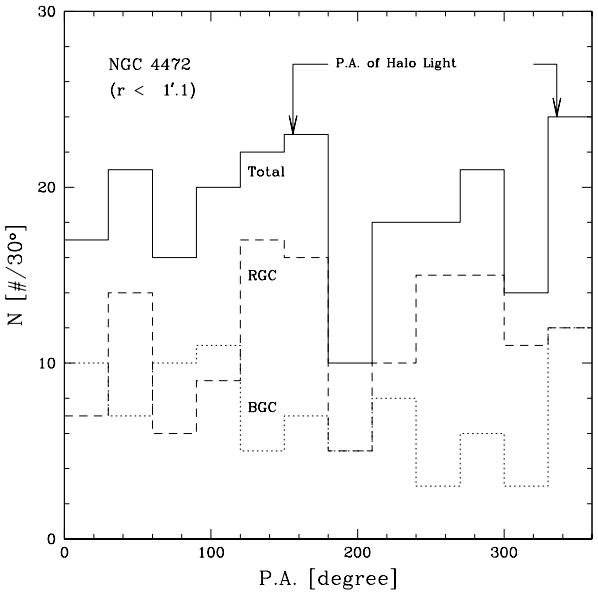

Fig. 22.— Azimuthal variation of the surface number density of the bright globular clusters with $V < 23.9$ mag in the region at $r < 1.1$ arcmin. The solid line, dotted line and dashed line show, respectively, the total sample, blue globular clusters, and red globular clusters.

TABLE 1
JOURNAL OF OBSERVATIONS FOR NGC 4472 IN THE HST ARCHIVE

Field	T_{exp}(F555W)	T_{exp}(F814W)	Date	Program ID and PI
C1 Field	2×900 s	2×900 s	1995 Feb. 4,5	GO.5236 Westphal
C2 Field	2×230 s	2×230 s	1995 Apr. 18	GO.5236 Westphal
N Field	900 s, 1300 s	900 s, 1400 s	1996 May 3	GO.5920 Brodie
S Field	900 s, 1300 s	900 s, 1400 s	1996 May 2	GO.5920 Brodie

TABLE 2
APERTURE CORRECTIONS

Field, Image	APC(F555W)	APC(F814W)
C1 Field		
PC	-0.434 ± 0.047	-0.626 ± 0.099
WF2	-0.202 ± 0.020	-0.257 ± 0.033
WF3	-0.213 ± 0.014	-0.261 ± 0.019
WF4	-0.182 ± 0.017	-0.239 ± 0.026
C2 Field		
PC	-0.522 ± 0.128	-0.658 ± 0.259
WF2	-0.190 ± 0.024	-0.252 ± 0.051
WF3	-0.217 ± 0.028	-0.289 ± 0.030
WF4	-0.195 ± 0.048	-0.225 ± 0.046
N Field		
PC	-0.506 ± 0.022	-0.541 ± 0.015
WF2	-0.205 ± 0.022	-0.244 ± 0.015
WF3	-0.206 ± 0.016	-0.280 ± 0.078
WF4	-0.267 ± 0.072	-0.314 ± 0.093
S Field		
PC	-0.667 ± 0.056	-0.851 ± 0.035
WF2	-0.259 ± 0.051	-0.263 ± 0.034
WF3	-0.251 ± 0.023	-0.292 ± 0.023
WF4	-0.245 ± 0.021	-0.263 ± 0.022

TABLE 3
COMPARISON OF THE PHOTOMETRY FOR THE OVERLAPPED REGIONS

Field	ΔV	N	ΔI	N
C1 Field(PC) minus C2 Field(PC)	0.017 ± 0.066	10	0.024 ± 0.032	10
C1 Field(WF2) minus C2 Field(WF4)	-0.001 ± 0.047	28	-0.043 ± 0.045	32
C1 Field(WF4) minus S Field(WF4)	-0.078 ± 0.061	5	0.009 ± 0.057	5
C2 Field(WF3) minus N Field(WF2)	0.011 ± 0.028	10	-0.028 ± 0.027	11
total objects	0.001 ± 0.049	52	-0.026 ± 0.051	59

TABLE 4

PHOTOMETRY OF BRIGHT GLOBULAR CLUSTERS WITH $V < 22$ MAG IN NGC 4472

ID	$\Delta RA('')^a$	$\Delta Dec('')^a$	V	$(V-I)$	$r('')$	ID	$\Delta RA('')^a$	$\Delta Dec('')^a$	V	$(V-I)$	$r('')$
1061	-91.3	-30.6	21.89	1.32	96.2	90	8.3	-109.6	21.58	0.89	109.9
617	-86.4	14.6	21.70	1.25	87.7	1246	12.0	-44.8	21.65	1.20	46.4
911	-78.6	-12.8	21.26	1.21	79.6	39	14.6	-138.1	21.69	1.33	138.9
741	-73.8	-1.8	20.45	1.24	73.8	23	19.4	-122.4	21.07	0.85	124.0
236	-69.3	21.0	21.87	1.16	72.4	179	19.6	-218.8	21.43	1.05	219.7
1062	-68.0	-44.6	21.83	1.18	81.3	371	20.6	-25.1	21.45	1.26	32.5
398	-67.0	12.8	21.82	1.07	68.2	514	25.6	65.0	19.82	1.01	69.9
417	-64.8	10.8	21.22	0.99	65.6	238	25.7	130.9	21.64	1.15	133.4
833	-64.5	-14.7	20.90	1.31	66.2	584	26.0	-19.5	21.62	0.93	32.5
1129	-64.1	-63.7	21.57	0.93	90.4	295	28.9	110.6	20.35	1.12	114.3
705	-60.2	-7.2	21.85	0.99	60.6	542	29.2	211.9	21.49	1.29	213.9
972	-55.9	-32.7	21.49	0.97	64.8	263	31.1	-193.2	21.54	1.25	195.7
233	-54.1	12.0	21.30	1.27	55.4	723	32.7	-26.2	21.25	1.04	41.9
925	-51.7	-30.5	20.40	1.12	60.0	243	33.7	28.1	20.78	0.96	43.8
772	-50.0	-18.1	21.47	1.11	53.1	541	34.3	75.8	21.54	1.00	83.2
749	-47.6	202.2	21.62	1.17	207.7	512	36.2	63.6	21.77	1.08	73.2
1153	-46.3	68.3	21.64	1.15	82.5	388	38.3	40.4	20.93	1.27	55.6
1084	-42.4	37.5	21.77	0.98	56.6	305	38.7	-177.3	21.64	0.92	181.5
256	-41.2	-36.6	21.69	1.30	55.1	417	40.7	95.1	21.60	1.09	103.5
314	-39.3	-0.1	20.03	1.19	39.3	327	42.8	-124.8	20.74	1.25	131.9
808	-38.8	-27.8	21.76	0.92	47.8	824	43.8	-4.8	21.21	1.12	44.1
648	-38.8	-15.6	21.51	0.95	41.8	379	44.4	39.4	21.26	1.32	59.3
480	-38.0	-128.3	21.07	0.98	133.8	503	45.5	61.5	21.43	0.95	76.5
1104	-36.2	54.0	21.43	1.28	65.0	549	48.4	79.5	21.76	0.97	93.1
617	-35.0	188.5	19.39	1.05	191.7	407	50.3	-179.5	21.85	0.96	186.4
450	-34.4	-8.7	21.78	1.20	35.4	432	51.0	140.6	20.74	0.95	149.6
347	-33.8	-4.7	20.92	0.93	34.1	99	52.1	20.0	21.40	0.99	55.8
402	-26.6	-106.2	21.68	1.25	109.5	368	55.2	38.1	21.16	1.03	67.1
467	-19.5	-20.3	20.31	1.13	28.2	259	61.4	159.9	21.88	1.21	171.3
322	-18.7	8.1	21.35	1.15	20.4	872	61.8	-22.7	21.52	1.14	65.8
1198	-18.4	-86.6	21.40	1.18	88.5	556	64.5	136.9	21.56	0.95	151.4
846	-16.5	-42.6	21.44	1.22	45.7	881	65.9	6.4	20.63	1.27	66.2
317	-16.2	-103.2	21.54	0.97	104.4	270	68.0	29.7	21.58	1.16	74.2
179	-15.6	9.5	20.25	1.19	18.2	142	69.2	21.8	20.59	0.97	72.6
441	-13.1	-170.3	21.52	1.14	170.8	554	69.9	81.4	21.70	0.99	107.3
766	-12.5	-30.1	21.87	1.08	32.6	427	71.0	43.9	20.48	1.11	83.5
905	-8.0	55.3	21.23	1.09	55.9	312	74.2	164.1	20.71	1.05	180.1
683	-7.6	-16.5	21.34	1.31	18.1	901	74.4	-43.8	21.78	0.91	86.3
60	-7.5	-7.9	21.13	1.26	10.9	902	75.9	0.3	21.08	1.36	75.9
344	-6.8	190.0	21.89	1.01	190.1	568	76.1	89.9	21.40	0.94	117.8
1289	-5.6	-87.7	21.85	1.37	87.9	419	76.5	43.0	21.68	1.28	87.7
1257	-3.9	-74.8	21.88	1.25	74.9	555	79.5	206.6	21.86	1.12	221.3
413	0.2	22.9	21.86	1.26	22.9	389	79.8	39.9	21.68	1.04	89.2
1199	0.7	-54.3	20.99	1.22	54.3	507	82.6	-110.7	21.88	1.22	138.1
339	3.1	31.6	21.46	1.30	31.8	911	83.9	-11.7	21.83	0.98	84.7
1366	4.3	-103.6	19.50	1.08	103.6	284	85.4	-137.2	21.82	1.32	161.6
292	4.6	32.3	21.82	1.27	32.6	499	85.5	191.5	21.48	1.02	209.8
79	6.9	-12.9	21.46	1.16	14.6	523	86.5	-109.2	20.23	1.02	139.3
1182	7.4	-39.4	21.43	0.92	40.1	265	88.7	155.9	20.79	1.08	179.3

[a] ΔRA, ΔDec, and r are calculated in the unit of arcsec with respect to the center of NGC 4472, for the position angle of the major axis of NGC 4472, 58.67 deg.

TABLE 5
LUMINOSITY FUNCTIONS OF THE GLOBULAR CLUSTERS IN NGC 4472

V	N(total)	N(BGC)	N(RGC)	V	N(total)	N(BGC)	N(RGC)
19.3	1	1	0	23.7	54	28	26
19.5	1	0	1	23.9	52	27	25
19.7	0	0	0	24.1	57	28	29
19.9	1	1	0	24.3	51	19	32
20.1	1	0	1	24.5	25	12	13
20.3	5	1	4	24.7	42	19	23
20.5	3	1	2	24.9	32	18	14
20.7	6	3	3	25.1	41	13	28
20.9	4	1	3	25.3	25	8	17
21.1	5	3	2	25.5	24	10	14
21.3	10	3	7	25.7	19	8	11
21.5	24	12	12	25.9	14	7	7
21.7	20	8	12	26.1	20	10	10
21.9	35	13	22	26.3	18	8	10
22.1	33	17	16	26.5	19	12	7
22.3	34	16	18	26.7	16	7	9
22.5	51	27	24	26.9	19	8	11
22.7	37	13	24	27.1	23	9	14
22.9	59	24	35	27.3	10	4	6
23.1	56	23	33	27.5	8	6	2
23.3	65	27	38	27.7	8	5	3
23.5	72	25	47	27.9	1	0	1

TABLE 6
LINEAR FITS OF MEAN MAGNITUDE PROFILES

SAMPLE		HST			HST+GROUND		
		Slope	Intercept	σ	Slope	Intercept	σ
Total	V	0.016 ± 0.039	22.491 ± 0.067	0.091	0.016 ± 0.007	22.475 ± 0.035	0.052
	I	0.035 ± 0.039	21.341 ± 0.067	0.098	0.026 ± 0.008	21.350 ± 0.035	0.058
BGC	V	0.042 ± 0.062	22.421 ± 0.105	0.083	0.024 ± 0.010	22.419 ± 0.050	0.052
	I	0.043 ± 0.063	21.449 ± 0.106	0.094	0.024 ± 0.010	21.447 ± 0.051	0.054
RGC	V	0.040 ± 0.050	22.474 ± 0.089	0.063	0.009 ± 0.011	22.523 ± 0.050	0.040
	I	0.045 ± 0.049	21.236 ± 0.088	0.065	0.013 ± 0.011	21.297 ± 0.050	0.043

TABLE 7
COLOR DISTRIBUTION OF THE GLOBULAR CLUSTERS WITH $V < 23.9$ MAG IN NGC 4472

$(V-I)$	N	$(V-I)$	N
0.625	1	1.125	68
0.675	5	1.175	58
0.725	4	1.225	68
0.775	4	1.275	65
0.825	11	1.325	53
0.875	24	1.375	15
0.925	65	1.425	8
0.975	74	1.475	1
1.025	59	1.525	1
1.075	53	1.575	0

TABLE 8
SURFACE NUMBER DENSITY OF THE GLOBULAR CLUSTERS WITH $V < 23.9$ MAG IN NGC 4472

r[arcmin]	σ_{GC}(total)	r[arcmin]	σ_{BGC}	r[arcmin]	σ_{RGC}
0.29	78.11 ± 12.35	0.33	25.04 ± 6.07	0.32	49.93 ± 9.12
0.48	71.79 ± 7.11	0.54	24.56 ± 3.67	0.55	41.80 ± 7.63
0.86	56.56 ± 5.60	0.96	20.87 ± 3.11	0.82	25.96 ± 4.72
1.18	45.93 ± 4.55	1.31	17.46 ± 2.60	1.13	27.41 ± 3.60
1.55	33.38 ± 3.31	1.72	15.95 ± 2.38	1.46	20.82 ± 2.73
2.17	29.58 ± 2.93	2.36	13.72 ± 2.05	2.04	16.21 ± 2.13
3.26	23.37 ± 2.35	3.33	10.80 ± 1.75	3.16	11.85 ± 1.58

[a] σ_{GC} is given in units of # arcmin^{-2}.

TABLE 9
COLOR PROFILES OF THE GLOBULAR CLUSTERS WITH $V < 23.9$ MAG IN NGC 4472

Total			BGC			RGC		
r (arcmin)	$V-I$ mean	$V-I$ median	r (arcmin)	$V-I$ mean	$V-I$ median	r (arcmin)	$V-I$ mean	$V-I$ median
0.413	1.131 ± 0.161	1.145	0.454	0.949 ± 0.080	0.977	0.385	1.237 ± 0.089	1.253
0.732	1.129 ± 0.151	1.155	0.786	0.974 ± 0.066	0.976	0.701	1.232 ± 0.081	1.232
0.991	1.140 ± 0.149	1.139	1.048	0.990 ± 0.053	0.985	0.955	1.234 ± 0.093	1.230
1.227	1.125 ± 0.140	1.121	1.304	0.966 ± 0.054	0.967	1.176	1.230 ± 0.086	1.240
1.479	1.100 ± 0.149	1.125	1.604	0.959 ± 0.067	0.951	1.415	1.219 ± 0.070	1.208
1.852	1.115 ± 0.154	1.121	2.043	0.953 ± 0.061	0.954	1.762	1.232 ± 0.075	1.235
2.477	1.085 ± 0.157	1.068	2.678	0.952 ± 0.061	0.948	2.355	1.234 ± 0.092	1.250
3.381	1.084 ± 0.130	1.064	3.462	0.978 ± 0.064	0.990	3.286	1.193 ± 0.078	1.196